

# The fundamental problem of treating light incoherence in photovoltaics and its practical consequences

Aline Herman<sup>†,1,\*</sup> Michaël Sarrazin<sup>†,1,†</sup> and Olivier Deparis<sup>†,1,‡</sup>

<sup>1</sup>*Solid-State Physics Laboratory, Research Center in Physics of Matter and Radiation (PMR),  
University of Namur, 61 rue de Bruxelles, B-5000 Namur, Belgium*

<sup>†</sup> *These authors have contributed equally to this work.*

The incoherence of sunlight has long been suspected to have an impact on solar cell energy conversion efficiency, although the extent of this is unclear. Existing computational methods used to optimize solar cell efficiency under incoherent light are based on multiple time-consuming runs and statistical averaging. These indirect methods show limitations related to the complexity of the solar cell structure. As a consequence, complex corrugated cells, which exploit light trapping for enhancing the efficiency, have not yet been accessible for optimization under incoherent light. To overcome this bottleneck, we developed an original direct method which has the key advantage that the treatment of incoherence can be totally decoupled from the complexity of the cell. As an illustration, surface-corrugated GaAs and c-Si thin-films are considered. The spectrally integrated absorption in these devices is found to depend strongly on the degree of light coherence and, accordingly, the maximum achievable photocurrent can be higher under incoherent light than under coherent light. These results show the importance of taking into account sunlight incoherence in solar cell optimization and point out the ability of our direct method in dealing with complex solar cells structures.

PACS numbers: 88.40.hj, 88.40.jj, 42.25.Kb

## I. INTRODUCTION

In photovoltaics, it has long been suspected that the incoherence of sunlight has an impact on the energy conversion efficiency of solar cells, although the extent of this is unclear. In photosynthesis, on the other hand, the incoherence of sunlight has been recently recognized to play a fundamental role on the optical-biological energy conversion process [1, 2].

The use of ultrathin (a few microns) crystalline Silicon (c-Si) active layers in solar cells is promising since it requires less material and therefore to decrease the costs. However, ultrathin layers result in drastic reduction of the absorption of the solar radiation in the near-infrared region due to the indirect band-gap of c-Si [3]. The efficiency of ultrathin solar cells is therefore limited. The use of optimized periodic photonic nanostructures (light-trapping structures) at the front and/or back-side(s) of the active layer of the solar cell is a promising approach to solve this issue [4–9]. This well-known design helps to couple incident light into the active layer via quasi guided modes [6–8, 10–12]. Most research focuses on finding the optimal structure geometry [13–18] that increases the absorption inside surface-corrugated ultrathin layers with the aim of reaching the fundamental upper bound limit on absorption [12, 19–24]. The determination of optimal light-trapping structures in ultrathin solar cells is therefore of high interest without loss of generality. This is the reason why we choose to focus here on the particularly relevant case of an ultrathin c-Si slab having its front side corrugated with periodic nanostructures (figure 1). Nevertheless, at present, the important issue of the plausible impact of sunlight incoherence on cell efficiency remains quite unexplored. Indeed, it is well known that the response of optical devices depends on the degree of coherence of the incident light [25]. Until now, the rarity of investigations in this area was related to the complexity of numerical methods dealing with incoherence. Methods addressing both spatial [26–34] or temporal [35] incoherence exist. The problem of incoherence seems, in principle, theoretically resolved. However, apart from experimental optimizations [36, 37], the theoretical optimization of complex solar cells (corrugated multilayers) under incoherent light has never been performed. This bottleneck is due to practical limitations of computational methods used to deal with incoherence. Simply stated, at each wavelength, multiple independent computational runs are performed and then statistically treated [35]. Each individual run consists of the resolution of Maxwell's equations in complex inhomogeneous media using Rigorous Coupled Wave Analysis (RCWA) [38–41] or Finite-Difference Time-Domain method (FDTD)[42, 43]. For each run,

---

\*Electronic address: aline.herman@unamur.be

†Electronic address: michael.sarrazin@unamur.be

‡Electronic address: olivier.deparis@unamur.be

the phase of the incident wave is randomly chosen [35]. Since the treatment of each wavelength needs multiple runs, the computational time demand is much more severe in the incoherent case than in the coherent one (where only one run is needed). Furthermore, as the complexity of the solar cell structure increases, the time required to compute one run increases dramatically. Therefore, because of both the complexity of the cell and the complexity of the algorithmic method, the accurate modelling of a complex solar cell under incoherent light becomes a formidable task. This is probably the reason why the effects of sunlight incoherence on complex solar cell efficiency have never been properly investigated.

In a recent article, we developed a rigorous theory accounting for the effects of temporal incoherence of light on the response of solar cells [44]. In the proposed method, a single time-consuming computation step is needed: the electromagnetic calculation of the coherent absorption spectrum. The incoherent absorption spectrum is then deduced directly through a convolution product with the coherent absorption spectrum. This second step is totally independent of the first one and therefore no multiple runs are needed at all. Our method is not only simpler than previous ones [26–35] but it also leads to a drastic reduction in computational time. Since the incoherent treatment (second step) is totally independent of the complexity of the solar cell structure, our method paves the route for extensive optimizations of solar cells under incoherent illumination.

In the present article, we show that the degree of sunlight coherence has a dramatical, unsuspected impact on the way solar cells should be optimized. Especially, we predict that the photocurrent produced by a corrugated thin-film solar cell strongly depends on the coherence time of the incident light. As an illustration, the maximum achievable photocurrent is numerically calculated in two types of uncoated corrugated semiconductor slabs, namely crystalline Silicon (c-Si) and Gallium Arsenide (GaAs), under exposure to incoherent light. The slabs have their top surfaces corrugated with wavelength-scale arrays of square or cylindrical holes for light trapping purposes. Though a real solar cell comprises more layers than the corrugated active material layer (antireflection coating, back reflector, electrodes etc.), the stand-alone corrugated slab is sufficient to highlight the effect of sunlight incoherence as it is intended here. The physical mechanism responsible for the dependence of the photocurrent on the degree of sunlight coherence is then discussed. Finally, we predict the potential gain in computational time thanks to the proposed method.

## II. OVERVIEW OF THE METHOD

A solar cell, like any optical-electrical energy conversion device, is at the same time a linear optical system as well as a photo-detector. Indeed, the cell performs light harvesting and, as in any linear system, is characterized by its transfer function (optical absorption spectrum here). The cell, on the other hand, collects electrons and holes which are generated by harvested photons. In comparison with the sunlight coherence time (estimated to 3 fs [45]), the detector response  $T$  is slow since typical carrier life time ranges from 0.1 ns to 1 ms in silicon, according to the doping level [46]. Therefore, it is crucial to consider the slowness of the detector response when averaging the solar cell response (photocurrent) under incoherent excitation.

The maximum achievable photocurrent  $J$  supplied by a solar cell is given by [47]:

$$J = \frac{e}{hc} \int A(\lambda)S(\lambda)\lambda d\lambda = \int J(\lambda)d\lambda \quad (1)$$

where  $e$  is the electron charge,  $h$  is the Planck's constant,  $c$  is the light velocity,  $A(\lambda)$  is the active layer absorption spectrum,  $S(\lambda)$  is the global power spectral density (PSD) of the solar radiation (AM1.5G spectrum) and  $J(\lambda)$  is the maximum achievable photocurrent spectrum. It should be noted that the only quantity that is detected by a solar cell is the integrated photocurrent  $J$ . Therefore, the numerical computation of the absorption spectrum is solely a computational step towards the determination of  $J$ . In order to take into account the incoherent nature of sunlight,  $A(\lambda)$  must represent the *effective* incoherent absorption  $A_{incoh}(\lambda)$  undergone by the solar cell. By *effective* absorption, we mean that  $A_{incoh}(\lambda)$  has to be considered as an intermediate quantity for calculating  $J$  (see later discussion related to figure 2). In numerous previously published works [11, 14–16, 48],  $A(\lambda)$  is actually the coherent absorption  $A_{coh}(\lambda)$  which is computed using numerical methods (RCWA, FDTD) that propagate the coherent electromagnetic field. In a few works, numerical methods were proposed in order to compute  $A_{incoh}(\lambda)$  [26–35]. However, they rely on multiple numerical runs, each one being performed for a coherent incident wave which is randomly dephased with respect to the previous one. The final result is then obtained from statistical averaging. Though correct, this procedure is time-consuming and not necessary as we show it hereafter. Recently, we have shown that  $A_{incoh}(\omega)$ , where  $\omega = 2\pi c/\lambda$  is the angular frequency, can be directly obtained from the convolution product (noted  $\star$ ) between  $A_{coh}(\omega)$  and an incoherence function  $I(\omega)$  [44]:

$$A_{incoh}(\omega) = I(\omega) \star A_{coh}(\omega). \quad (2)$$

The incoherence function is defined by the Gaussian distribution [44]:

$$I(\omega) = \tau_c \sqrt{\frac{\ln 2}{\pi^3}} e^{-\frac{\ln 2}{\pi^2} \tau_c^2 \omega^2} \quad (3)$$

with a Full Width at Half Maximum  $\Delta\omega = 2\pi/\tau_c$  inversely related to the coherence time  $\tau_c$ . Physically,  $I(\omega)$  describes the stochastic behaviour of each spectral line (optical carrier at frequency  $\omega$ ) composing the whole solar spectrum. This formula is easy to use in practice and allows to reduce the algorithm complexity, hence the computational time. Full rigorous demonstration of (2) was given in [44]. Nevertheless, in order to understand the physics behind the convolution formula, we present a simplified version of the method reported in [44].

### III. THEORETICAL FRAMEWORK OF THE METHOD AND PHYSICAL INTERPRETATION

Though Maxwell's equations are linear, addressing the issue of the power flux absorbed by a linear system under incoherent excitation is not a trivial problem as we will see in the following sections. In the frame of random signal theory, we demonstrate hereafter that the incoherent output power of a linear system can be obtained from the coherent output power. This general result applies to solar cells in particular, where the incident sunlight is temporally incoherent, i.e. each frequency component of the solar spectrum can be regarded as a random process. Since all random processes related to each optical carrier frequency are independent, each carrier frequency can be treated individually.

#### A. Basic concepts in random signal theory

Hereafter, we present briefly basic concepts in random signal theory such as autocorrelation, PSD and normalized power (we follow the notation of [49]). The real stationary random signal we consider is noted  $x(t)$ . In the particular case of solar cells,  $x(t)$  is the electric field of the electromagnetic radiation. The autocorrelation function of the random signal is defined as [49]

$$R_X(\tau) = E[x(t)x(t + \tau)], \quad (4)$$

where  $E[\cdot]$  denotes the expectation value of  $x(t)$  (i.e. ensemble average). When  $\tau = 0$ , we find the mean square value of the signal:

$$R_X(0) = E[x^2(t)]. \quad (5)$$

In the context of solar cells, this quantity is proportional to the average power transported by the optical wave at the carrier frequency  $\omega_c$ . The Power Spectral Density (PSD)  $S_X(\omega)$ , is defined as the Fourier transform of  $R_X(\tau)$ :

$$S_X(\omega) = \int_{-\infty}^{\infty} R_X(\tau) e^{i\omega\tau} d\tau. \quad (6)$$

However, for a stationary random signal expanding from  $-\infty$  to  $\infty$  in time, the function  $R_X$  is not integrable [49]. Thus, the Fourier transform (hence PSD) does not converge. In order to define the PSD of a random signal, the signal must be truncated within a span of time  $T$ , i.e. the sampling interval [49]. The truncated signal is noted by  $x_T(t)$ , with  $x_T(t) = x(t)$  over time span  $T$  and  $x_T(t) = 0$  elsewhere. Thanks to truncation, the Fourier transform can be defined for each realization  $x_T(t)$  of the signal. The stochastic quantity corresponding to the Fourier transform of the truncated signal is defined by:

$$X(\omega) = \mathcal{F}[x_T(t)], \quad (7)$$

where  $\mathcal{F}$  is the Fourier transform. For large  $T$ , it can be shown [49] that

$$S_X(\omega) = E \left[ \frac{1}{T} |X(\omega)|^2 \right]. \quad (8)$$

Using the PSD, we can then define the normalized average power as

$$P_X = R_X(0) = \frac{1}{2\pi} \int_{-\infty}^{\infty} S_X(\omega) d\omega = E \left[ \frac{1}{T} \frac{1}{2\pi} \int_{-\infty}^{\infty} |X(\omega)|^2 d\omega \right]. \quad (9)$$

From a physical point of view, (9) simply means that the integration of the PSD yields the power.

In the context of solar cells, the sampling time  $T$  is effectively the photo-detector response time which is very long at the time scale of the random process. Therefore, the assumption of large  $T$  in (8) is fully satisfied. Note that, in the scattering matrix treatment of (2), the detector response was lumped in the time averaged Poynting vector flux expression in the form of a narrow bandwidth filtering function ((A26) to (A29) in [44]).

Hereafter, we consider a linear system subject to both coherent or incoherent input signals and we calculate the corresponding output signals.

### B. Coherent signal output

The coherent input signal  $x_{in}^{coh}(t)$  is taken to be a real cosine function:

$$x_{in}^{coh} = E_0 \cos(\omega_c t), \quad (10)$$

where  $E_0$  is the amplitude of the signal and  $\omega_c$  is the carrier frequency. According to (4), we find

$$R_{x,in}^{coh}(\tau) = \frac{|E_0|^2}{2} \cos(\omega_c \tau). \quad (11)$$

Since the coherent input power corresponds to  $R_{x,in}^{coh}(\tau = 0)$ , we have the well known result:

$$P_{x,in}^{coh} = \frac{|E_0|^2}{2}. \quad (12)$$

According to linear system theory [49] applied to deterministic signals, the coherent output power is given by:

$$P_{x,out}^{coh} = |G(\omega_c)|^2 P_{x,in}^{coh} = |G(\omega_c)|^2 \frac{|E_0|^2}{2}, \quad (13)$$

where  $G(\omega_c)$  is the transfer function of the system under study at frequency  $\omega_c$ .

### C. Incoherent signal output

The incoherent input signal  $x_{in}^{incoh}(t)$  is expressed as a carrier whose amplitude is randomly modulated:

$$x_{in}^{incoh}(t) = E_0 m(t) e^{-i\omega_c t}, \quad (14)$$

where  $m(t)$  represents the random process (modulation function) and  $e^{-i\omega_c t}$  is the periodic component of the signal at the carrier frequency. The complex form of (14) is simply used for the sake of simplicity in the mathematical derivation. Of course, we implicitly work with the real part of (14).

The Fourier transform of the random input signal is

$$X_{in}^{incoh}(\omega) = E_0 M(\omega - \omega_c), \quad (15)$$

where  $M(\omega)$  is the Fourier transform of  $m(t)$ . Using (9) and (15), we find for the incoherent input power:

$$P_{x,in}^{incoh} = |E_0|^2 E \left[ \frac{1}{T} \frac{1}{2\pi} \int_{-\infty}^{\infty} |M(\omega - \omega_c)|^2 d\omega \right]. \quad (16)$$

According to (8), we rewrite (16) as:

$$P_{x,in}^{incoh} = \frac{|E_0|^2}{2\pi} \int_{-\infty}^{\infty} S_M(\omega - \omega_c) d\omega, \quad (17)$$

where

$$S_M(\omega) = E \left[ \frac{1}{T} |M(\omega)|^2 \right], \quad (18)$$

is the PSD of the random process, an even function of  $\omega$  [49]. Since both incoherent and coherent input signals must have the same power (i.e.  $P_{x,in}^{coh} = P_{x,in}^{incoh}$ ),  $S_M(\omega)$  must verify the normalization relation:

$$\int_{-\infty}^{\infty} S_M(\omega) d\omega = \pi. \quad (19)$$

Now, let us calculate the incoherent output power ( $P_{x,out}^{incoh}$ ). Using (9), we get:

$$P_{x,out}^{incoh} = E \left[ \frac{1}{T} \frac{1}{2\pi} \int_{-\infty}^{\infty} |X_{out}^{incoh}(\omega)|^2 d\omega \right] \quad (20)$$

According to linear system theory, the Fourier transform of the output signal is related to the Fourier transform of the input signal through the transfer function [49]:

$$X_{out}(\omega) = G(\omega)X_{in}(\omega). \quad (21)$$

Then, it follows from (20) and (21) that

$$P_{x,out}^{incoh} = E \left[ \frac{1}{T} \frac{1}{2\pi} \int_{-\infty}^{\infty} |G(\omega)|^2 |X_{in}^{incoh}(\omega)|^2 d\omega \right]. \quad (22)$$

Using (15) and (22) we get:

$$P_{x,out}^{incoh} = \frac{|E_0|^2}{2\pi} E \left[ \frac{1}{T} \int_{-\infty}^{\infty} |G(\omega)|^2 |M(\omega - \omega_c)|^2 d\omega \right] \quad (23)$$

$$= \frac{|E_0|^2}{2\pi} E \left[ \frac{1}{T} |G(\omega_c)|^2 \star |M(\omega_c)|^2 \right] \quad (24)$$

$$= \frac{|E_0|^2}{2\pi} |G(\omega_c)|^2 \star E \left[ \frac{1}{T} |M(\omega_c)|^2 \right]. \quad (25)$$

The symbol  $\star$  designates the convolution product. Using (18), we get:

$$P_{x,out}^{incoh} = \frac{|E_0|^2}{2\pi} |G(\omega_c)|^2 \star S_M(\omega_c). \quad (26)$$

Considering the expression of the coherent output power (13), we find the relationship between the incoherent output power and the coherent one:

$$P_{x,out}^{incoh}(\omega_c) = \frac{1}{\pi} P_{x,out}^{coh}(\omega_c) \star S_M(\omega_c). \quad (27)$$

Finally, using the normalization relation (19), we find the most important formula of this paper:

$$P_{x,out}^{incoh}(\omega_c) = P_{x,out}^{coh}(\omega_c) \star I(\omega_c), \quad (28)$$

where

$$I(\omega) = \frac{S_M(\omega)}{\int_{-\infty}^{\infty} S_M(\omega) d\omega}. \quad (29)$$

As a consequence, the power of the incoherent output signal is equal to the power of the coherent output signal that is convoluted with the PSD of the random process.

Equation (28) is formally equivalent to (2) which was derived in [44]. However, in the present case, we have only considered the transfer function of a linear system relating a single input channel to a single output channel. This formalism obviously does not allow to calculate optical reflectance ( $R$ ), transmittance ( $T$ ) or absorption ( $A = 1 - R - T$ ). In order to calculate these quantities, we must use the scattering matrix of the system instead of its transfer function. In this case, the derivation of (2) is more complicated (see [44] for details) but ends up with a formula equivalent to (28). It should be noted that a result similar to (28) was reported for the description of vibrational random processes [50]. Surprisingly, albeit fundamental, the theory of linear system response to stochastic signals appears to have remained rather confidential until now, at least in the field of photovoltaics.

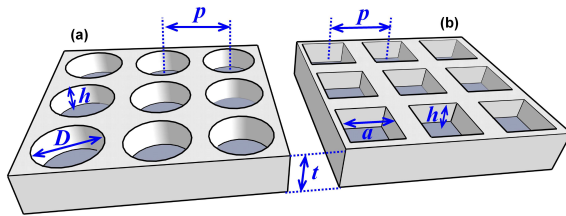


FIG. 1: (Colour online). Corrugated slabs (i.e. active layers of thin-film solar cells).  $t$ : slab thickness,  $h$ : height of holes,  $p$ : period of hole array.  $D$ : diameter of cylindrical holes (a).  $a$ : side of square holes (b).

#### IV. ILLUSTRATION OF THE METHOD

Using the above described theoretical method, we now investigate the effect of finite temporal coherence of the sunlight on the efficiency of solar cells. Under coherent illumination, the type of front-side corrugation is known to have a strong influence on the photocurrent [15, 16, 48]. Therefore, it is important to properly optimize the corrugation (we do not consider here additional improvements brought by conformal antireflection coating and/or back reflector). In order to investigate the impact of the coherence time on such an optimization, we studied two different corrugations, with cylindrical or square holes (figure 1).

Both corrugated slabs have fixed thickness ( $t = 1\mu\text{m}$ ) and fixed hole depth ( $h = 500\text{nm}$ ). Slab thickness and hole depth are typical of ultrathin solar cell designs where photonic light trapping effects are exploited [12, 16]. The ratio between hole size (diameter  $D$  or side  $a$ ) and period ( $p$ ) has a fixed value equal to 0.9. These values result from previous optimization studies [16]. The period is the only varying parameter (from 250nm to 1250nm). Two types of materials are investigated: crystalline silicon (c-Si) and gallium arsenide (GaAs). The holes are supposed to be filled with air (i.e. incidence medium). The aim here is not to find again the best corrugation shape (cf. [16]) but to highlight the effect of coherence time for different shapes.

The photocurrent (1) under incoherent illumination was calculated for various coherence times (integration carried out from  $\lambda = 200\text{nm}$  to  $2500\text{nm}$ ). Under incoherent illumination,  $A(\lambda)$  was equal to  $A_{incoh}(\lambda)$  which was deduced from  $A_{coh}(\lambda)$  using (2). The coherent absorption spectrum was numerically calculated using the RCWA method. In (1), the rate of incident photons (per unit area) at each carrier wavelength was fixed by the intensity of the corresponding frequency-resolved component of the AM1.5 solar power density spectrum. The incident light was supposed to be unpolarized and impinging under normal incidence.

Before studying the photocurrent dependence on the coherence time, let us consider incoherent effects from a quantum mechanical point of view by resorting to Heisenberg's uncertainty principle. Due to their finite coherence time, each photon from the solar radiation cannot be defined with a definite energy  $E_0$  (or carrier wavelength  $\lambda_0 = hc/E_0$ ). According to Heisenberg's uncertainty principle:

$$\Delta E \Delta t \geq \frac{\hbar}{2}, \quad (30)$$

each photon is characterized by a spectral width  $\Delta E$  with a time uncertainty  $\Delta t \approx \tau_c$  related to the coherence time, i.e. each photon is treated as a wave packet. Accordingly, each photon has finite coherence length, i.e.  $l_c = c\tau_c$ . From (30), we must consider that a photon wave packet with a carrier wavelength  $\lambda_0$  occupies a spectral domain roughly defined by  $\mathcal{D}_s \sim [\lambda_0 - \Delta\lambda, \lambda_0 + \Delta\lambda]$  with  $\Delta\lambda \approx \lambda_0^2/(4\pi c\tau_c)$ . It means that the photon does not feel a single value of the complex refractive index  $n(\lambda_0) + ik(\lambda_0)$ , but a range of values  $n(\lambda) + ik(\lambda)$  with  $\lambda \in \mathcal{D}_s$  (remember that  $k$  is the material extinction coefficient responsible for optical absorption). As a consequence, even if  $k(\lambda_0)$  is almost equal to zero, namely above the bandgap wavelength ( $\lambda_g \approx 1.1\mu\text{m}$  for c-Si), the photon, as a wave packet, can be absorbed provided that  $k(\lambda) \neq 0$  on  $\mathcal{D}_s$ . It does not mean, however, that absorption occurs below the energy bandgap ( $\lambda_0 > \lambda_g$ ). Only available energy quanta from the wave packet ( $\lambda \in \mathcal{D}_s$ ) which are above the bandgap ( $\lambda < \lambda_g$ ) are absorbed and generate electron-hole pair. As an illustration, let us consider a carrier wavelength equal to  $\lambda_0 = 1700\text{nm}$  for which  $k(\lambda_0) \approx 0$  ( $\lambda_0 > \lambda_g$ ).

In the coherent case, when the perfectly coherent limit is reached (i.e.  $\tau_c \rightarrow \infty$ ), the incoherence function  $I(\lambda)$  becomes a Dirac function centered at  $\lambda_0 = 1700\text{nm}$ . At  $\lambda_0 = 1700\text{nm}$ , the computed coherent absorption is almost equal to zero. Accordingly, the coherent photocurrent is also almost equal to zero at that wavelength. In the incoherent case, the spectral width of the incoherence function  $I(\lambda)$  increases as the coherence time decreases (figure 2(a)). Therefore, a wider range of wavelengths enters into the calculation, including shorter wavelengths that are absorbed by the material (i.e.  $k \neq 0$ ). Physically, as explained above, this arises from the fact that a time-truncated sinusoidal signal ( $\Delta t \approx \tau_c$ ), i.e. a burst of signal with finite coherence time, becomes a polychromatic signal (with

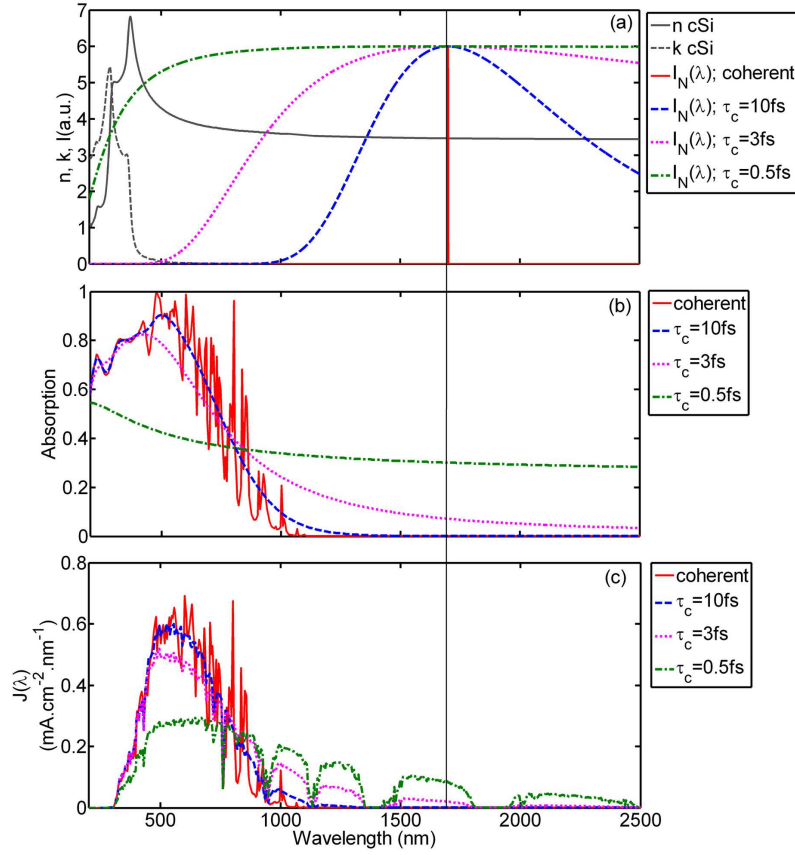


FIG. 2: (Colour online). (a) Real (grey black line) and imaginary (dotted grey line) parts of c-Si refractive index as function of wavelength. Normalized incoherence function  $I(\lambda)$  for various coherence times: coherent case (solid red line),  $\tau_c = 10$ fs (dashed blue line), 3fs (dotted magenta line) and 0.5fs (dashed-dotted green line).  $I(\lambda)$  is centered around  $\lambda_0 = 1700$ nm for illustrative purpose. (b) Absorption spectra in a  $1 \mu\text{m}$ -thick c-Si slab with cylindrical holes ( $p = 450$ nm) for various coherence times: coherent case (solid red line), 10fs (dashed blue line), 3fs (dotted magenta line) and 0.5fs (dashed-dotted green line). (c) Corresponding photocurrent spectra  $J(\lambda)$  for the same values of coherence time.

a width  $\Delta E$ ). In other words, while the carrier sinusoidal wave is at  $\lambda_0 = 1700$ nm, the incoherent wave packet contains shorter wavelengths which can be absorbed. As a consequence, the whole spectral range weighted by the incoherence function must be considered to compute the incoherent absorption  $A_{incoh}(\lambda_0)$ . This explains why the incoherent absorption increases around 1700nm as the coherence time decreases. Conversely, a wavelength (e.g.  $\lambda_0 = 500$ nm) that is strongly absorbed in the coherent case can lead to a lower absorption in the incoherent case. This is due to the fact that longer wavelengths experiencing  $k \approx 0$  come to play when determining the incoherent absorption. Mathematically, the above physical considerations translate into the convolution product of (2). As a result, the increase or decrease of the absorption at a specific wavelength affects the photocurrent  $J(\lambda)$  as  $\tau_c$  varies. For instance, at  $\lambda_0 = 1700$ nm, no photocurrent is generated in the coherent case. However, as  $\tau_c$  decreases,  $J(\lambda_0)$  increases. On the other hand, at  $\lambda_0 = 500$ nm, a high photocurrent is achieved in the coherent case. However, as  $\tau_c$  decreases,  $J(\lambda_0)$  decreases. Since the total (integrated) photocurrent  $J = \int J(\lambda)d\lambda$  is obtained by integrating over a wide range of wavelengths, it can increase or decrease according to the values of  $\tau_c$  (see trends in figure 5 below).

Maps of the photocurrent  $J$  were computed for both slabs defined in figure 1 with c-Si or GaAs as active material, according to various periods, coherence times and coherence lengths (figure 3). The analysis of  $J$  according to the period can be followed either in terms of coherence time ( $\tau_c$ ) or coherence length ( $l_c$ ). The use of  $l_c$  enables the comparison between the optimal period and the estimated coherence length of sunlight. The permittivities of materials were taken from the literature [51]. The aim is to highlight the effect of coherence time on the efficiency. However, it should be noted that the relevant values in figure 3 are those corresponding to  $\tau_c$  around 3fs (estimated coherence time of sunlight [45]). In order to highlight differences between  $J_{coh}$  and  $J_{incoh}$ , we plotted the graphs of the photocurrent ( $J$ ) versus the period for either asymptotically coherent light ( $\tau_c = 100$ fs) or incoherent sunlight ( $\tau_c = 3$ fs) (figure 4).

Two optimal periods (i.e. maximizing the photocurrent) are found for the c-Si slab corrugated with cylindrical

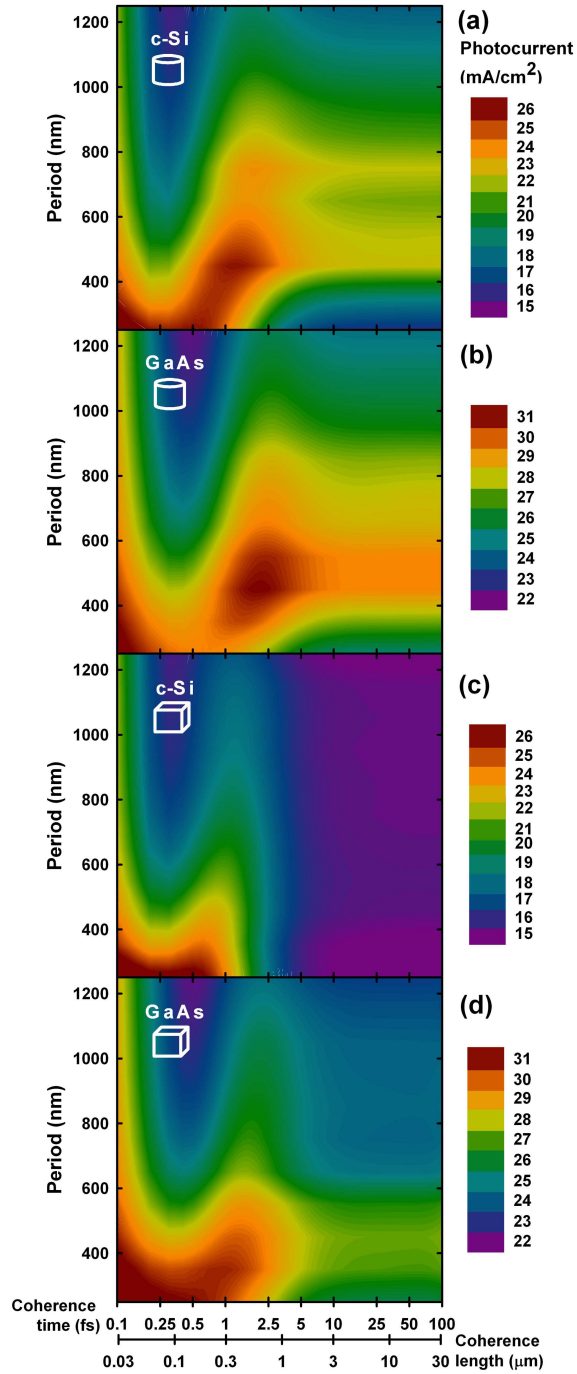


FIG. 3: (Colour online). Photocurrent vs. corrugation period, coherence time or length. Cylindrical holes in c-Si (a) or GaAs (b). Square holes in c-Si (c) or GaAs (d).

holes and illuminated under coherent light:  $p = 450\text{nm}$  and  $750\text{nm}$  (figure 3(a) and figure 4). If we only think in terms of coherent light, we could use both optima since they lead to the same photocurrent. However, when  $\tau_c$  decreases, we notice that  $J$  depends strongly on  $\tau_c$  (figure 3(a)). In a general way, we notice that, depending on the degree of coherence, a structure could be optimized under coherent light (i.e. high values of  $\tau_c$ ) while remaining optimal or being better or worse under incoherent light (figure 3). Therefore, the choice of the optimal corrugation (period and hole shape) strongly depends on  $\tau_c$ . An optimal structure under coherent light is not necessarily the optimal one under incoherent light, and vice versa. For a coherence time equal to  $3\text{fs}$  (estimated sunlight coherence time [45]), in the four cases (GaAs or c-Si corrugated with square or cylindrical holes), the photocurrent is higher

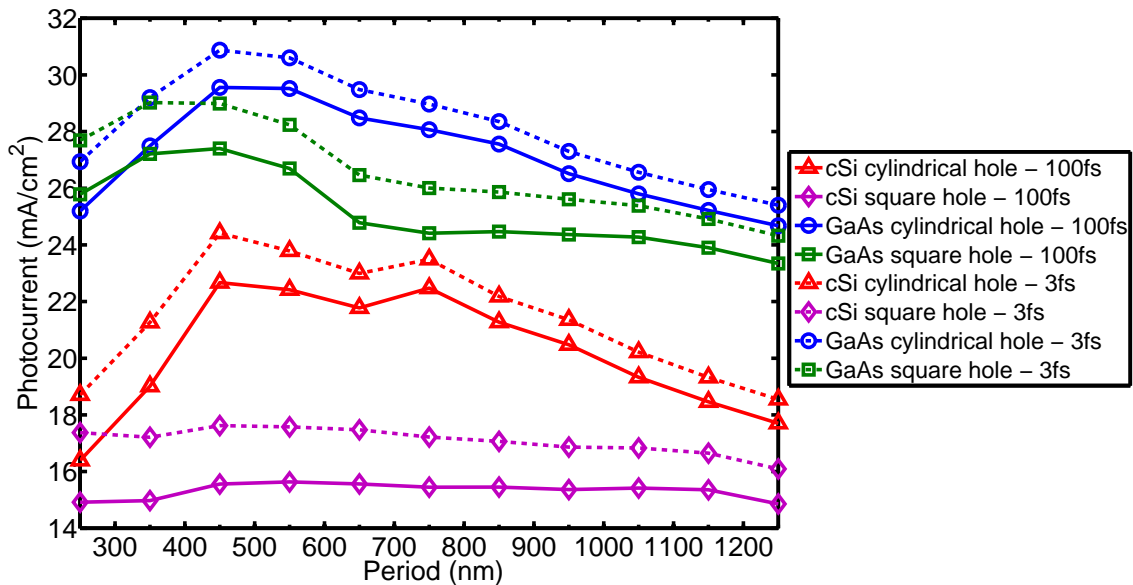


FIG. 4: (Colour online). Photocurrent versus period in the (asymptotical) coherent case ( $\tau_c = 100\text{fs}$ , solid lines) and in the incoherent case ( $\tau_c = 3\text{fs}$ , dashed lines) for GaAs slab corrugated with cylindrical holes (circle and blue lines) or square holes (square and green lines) and for c-Si slab corrugated with cylindrical holes (triangle and red lines) or square holes (diamond and magenta lines).

in the incoherent case than in the coherent case (figure 4). Therefore, photocurrent under sunlight could be higher than under hypothetical coherent light. This kind of behaviour has recently been observed by Abass et al. [34]. The choice of the optimal corrugation also depends on the material used in the active layer. For both materials, when the shape of the holes changes from cylinder to square, the optima shift to smaller coherence times (figure 3). Since the photocurrent is strongly influenced not only by the hole shape [16] but also by the coherence time, it turns out to be necessary to optimize light trapping structures taking also into account the coherence time of the solar radiation, which is not currently done in literature.

In order to better understand the influence of  $\tau_c$  on  $J$ , we plotted a cross-section of the maps of figure 3 for  $p = 450\text{nm}$  (figure 5). This period is not the optimal one for the four studied structures. However, it is a compromise since  $J$  is high for the four structures under coherent illumination. Figure 5 shows that the photocurrent is quite constant at long coherence times. As  $\tau_c$  decreases, however,  $J$  increases, reaches a maximum, decreases and then increases again.

Recently, researchers have investigated the effects of disorder in advanced photonic nanostructures surrounding the active layer of solar cells. These structures typically consist of complex unit cells (called super-cells) in which the nanostructure features are pseudo-randomly positioned [52–58]. They reached the conclusion that these kinds of disordered nanostructures could increase further (in comparison with periodic nanostructures) the absorption inside the active layer. Further investigations of the impact of finite coherence time/length on disordered structures would be of high interest for future solar cell optimization.

## V. ESTIMATION OF THE POTENTIAL GAIN IN COMPUTATIONAL TIME

The obvious advantage of our direct method is the potential gain in computational time it offers in comparison with a multiple-run approach. Indeed, the use of the convolution formula (2) in the integrated photocurrent expression (1) allows us to account for incoherence without the need for multiple time-consuming numerical runs and subsequent statistical analysis. In order to estimate the potential gain in computational time, let us consider as an example the  $1\mu\text{m}$ -thick c-Si slab corrugated with cylindrical holes. In our RCWA calculation,  $11 \times 11$  plane waves (diffraction orders) were used to reach good numerical convergence. On our computational cluster [59], the calculation of the coherent absorption at a single wavelength took  $t_\lambda = 7.5$  s. The whole spectrum (1000 wavelengths) took therefore  $t_{1000\lambda} = 7500$  s. The convolution took only a few minutes ( $t_{convol}$ ) on a personal computer. For this calculation to be performed for 10 grating periods (figure 4) took  $t_{tot} \approx 10 \times t_{1000\lambda} \approx 21$  h. If we would have used a multiple-run approach,  $t_\lambda$  would have been multiplied by  $N$ , the number of runs. In Lee’s method [35], 100 runs were needed for

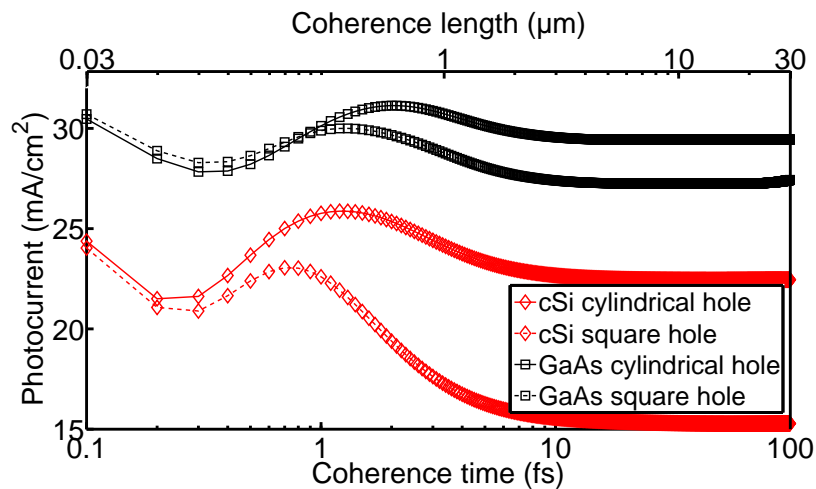


FIG. 5: (Colour online). Photocurrent versus the coherence time/length for GaAs (square and black lines) and for c-Si (diamond and red lines) slabs corrugated with cylindrical holes (solid lines) or square holes (dashed lines). In all cases,  $p = 450\text{nm}$  and  $t = 1\mu\text{m}$ .

each wavelength. It would have implied a multiplication of the computational time  $t_{tot}$  by a factor  $N$ :  $t_{tot} = 100 \times 21 \text{ h} \approx 87 \text{ days}$ . Furthermore, as the complexity of the solar cell structure increases,  $t_\lambda$  increases by orders of magnitude and therefore the total computational time  $t_{tot}$  clearly becomes dissuasive using a multiple-run approach.

## VI. CONCLUSION

Using the theory of random signals applied to linear systems, we demonstrated that the effective incoherent absorption spectrum of a solar cell can be directly calculated from the coherent one. This theoretical result has a significant impact on the optimization of solar cells. Indeed, in comparison with current numerical methods based on multiple computational runs and statistical averaging, the treatment of incoherence is shown here to no longer be related to the complexity of the cell structure, which saves a lot of computational time in many cases. The considerable simplification of the problem gives the opportunity to optimize theoretically complex solar cells under incoherent light which has been out of reach so far.

In a typical light trapping scheme based on periodic surface corrugations, we proved that the coherence time of the light illuminating the solar cell influences drastically the maximum achievable photocurrent. Depending on the shape of the surface corrugation and on the active layer material, the photocurrent may increase or decrease as the coherence time changes. In the four cases discussed in this article, the photocurrent under sunlight turns out to be higher than under coherent light. Such a result is fundamentally related to Heisenberg uncertainty principle and shows that solar cell efficiency may be enhanced when taking into account light incoherence. In other words, an optimal solar cell structure under coherent illumination is not necessarily an optimal one under incoherent illumination and vice versa. The optimization of a solar cell must therefore be performed in future by taking into account light incoherence, and not coherent illumination as has usually been done previously. Such a task is no longer a bottleneck since the time-consuming coherent response calculation only needs to be performed once for all and the incoherent response can be deduced directly from the convolution product with the power spectral density of the random process.

## Acknowledgements

The authors acknowledge J.P. Vigneron for useful discussions and comments. M.S. is supported by the Cleanoptic project (Development of super-hydrophobic anti-reflective coatings for solar glass panels / Convention No.1117317) of the Greenomat program of the Wallonia Region (Belgium). O.D. acknowledges the support of FP7 EU-project No.309127 PhotoNVoltatics (Nanophotonics for ultra-thin crystalline silicon photovoltaics). This research used resources of the “Plateforme Technologique de Calcul Intensif” (PTCI) (<http://www.ptci.unamur.be>) located at the University of Namur, Belgium, which is supported by the F.R.S.-FNRS. The PTCI is member of the “Consortium

des Equipements de Calcul Intensif (CECI)” (<http://www.ceci-hpc.be>).

- 
- [1] Manal T and Valkunas L 2010 *New Journal of Physics* **12** 065044
- [2] Kassal I, Yuen-Zhou J and Rahimi-Keshari S 2013 *The Journal of Physical Chemistry Letters* **4** 362–367
- [3] Muller J, Rech B, Springer J and Vanecek M 2004 *Solar Energy* **77** 917 - 930
- [4] Tsakalacos L 2010 *Nanotechnology for Photovoltaics* (Boca Raton: CRC Press)
- [5] Nelson J 2003 *The Physics of Solar Cells* (London: Imperial College)
- [6] Zeman M, Van Swaaij R. A. C. M. M, Metselaar J. W and Schropp R 2000 *Journal of Applied Physics* **88** 6436–6443
- [7] Campbell P and Green M. A 1987 *Journal of Applied Physics* **62** 243–249
- [8] Yablonovitch E and Cody G 1982 *IEEE Transactions on Electron Devices* **29** 300–305
- [9] Abass A, Le K. Q, Alù A, Burgelman M and Maes B 2012 *Physical Review B* **85** 115449
- [10] Saeta P. N, Ferry V. E, Pacifici D, Munday J. N and Atwater H. A 2009 *Optics Express* **17** 20975–20990
- [11] Gomard G, Drouard E, Letartre X, Meng X, Kaminski A, Fave A, Lemiti M, Garcia-Caurel E and Seassal C 2010 *Journal of Applied Physics* **108** 123102
- [12] Yu Z, Raman A and Fan S 2012 *Physical Review Letters* **109** 173901
- [13] Sigmund O and Hougaard K 2008 *Physical Review Letters* **100** 153904
- [14] Gjessing J, Marstein E. S and Sudbø A 2010 *Optics Express* **18** 5481–5495
- [15] Bozzola A, Liscidini M and Andreani L. C 2012 *Optics Express* **20** A224–A244
- [16] Herman A, Trompoukis C, Depauw V, El Daif O and Deparis O 2012 *Journal of Applied Physics* **112** 113107
- [17] Jovanov V, Xu X, Shrestha S, Schulte M, Hupkes J, Zeman M and Knipp D 2013 *Solar Energy Materials and Solar Cells* **112** 182–189
- [18] Lockau D, Sontheimer T, Becker C, Rudigier-Voigt E, Schmidt F and Rech B 2013 *Optics Express* **21** A42–A52
- [19] Yu Z, Raman A and Fan S 2010 *Optics Express* **18** A366–A380
- [20] Niv A, Gharghi M, Gladden C, Miller O. D and Zhang X 2012 *Physical Review Letters* **109** 138701
- [21] Markvart T and Bauer G. H 2012 *Applied Physics Letters* **101** 193901
- [22] Mellor A, Tobas I, Mart A, Mendes M and Luque A 2011 *Progress in Photovoltaics: Research and Applications* **19** 676687
- [23] Naqavi A, Haug F.-J, Battaglia C, Herzig H. P and Ballif C 2013 *JOSA B* **30** 1320
- [24] Naqavi A, Haug F.-J, Söderström K, Battaglia C, Paeder V, Scharf T, Herzig H. P and Ballif C 2013 *Progress in Photovoltaics: Research and Applications* published online
- [25] Born M and Wolf E 1999 *Principles of optics* (Cambridge: Cambridge University Press)
- [26] Mitsas C. L and Siapkas D. I 1995 *Applied optics* **34** 16781683
- [27] Prentice J. S. C 1999 *Journal of Physics D: Applied Physics* **32** 2146
- [28] Prentice J. S. C 2000 *Journal of Physics D: Applied Physics* **33** 3139
- [29] Katsidis C. C and Siapkas D. I 2002 *Applied optics* **41** 39783987
- [30] Centurioni E 2005 *Applied optics* **44** 75327539
- [31] Troparevsky M. C, Sabau A. S, Lupini A. R and Zhang Z 2010 *Optics Express* **18** 24715–24721
- [32] Krč J, Smole F and Topič M 2003 *Progress in Photovoltaics: Research and Applications* **11** 1526
- [33] Santbergen R, Smets A. H and Zeman M 2013 *Optics Express* **21** A262–A267
- [34] Abass A, Trompoukis C, Leyre S, Burgelman M and Maes B 2013 *Journal of Applied Physics* **114** 033101
- [35] Lee W, Lee S.-Y, Kim J, Kim S. C and Lee B 2012 *Optics express* **20** A941A953
- [36] Sai H, Saito K and Kondo M 2012 *Applied Physics Letters* **101** 173901
- [37] Sai H, Saito K, Hozuki N and Kondo M 2013 *Applied Physics Letters* **102** 053509
- [38] Moharam M. G and Gaylord T. K 1981 *JOSA* **71** 811818
- [39] Sarrazin M, Vigneron J.-P and Vigoureux J.-M 2003 *Physical Review B* **67** 085415
- [40] Vigneron J.-P, Forati F, Andre D, Castiaux A, Derycke I and Dereux A 1995 *Ultramicroscopy* **61** 21–27
- [41] Vigneron J. P and Lousse V 2006 *SPIE Proceedings* vol 6128 (SPIE) p 61281G
- [42] Kunz K. S and Luebbers R. J 1993 *The finite difference time domain method for electromagnetics* (Boca Raton: CRC Press)
- [43] Taflove A and Hagness S. C 2005 *Computational electrodynamics: the finite-difference time-domain method* (Boston: Artech House)
- [44] Sarrazin M, Herman A and Deparis O 2013 *Optics Express* **21** A616
- [45] Hecht E 2002 *Optics* (San Francisco: Pearson Education)
- [46] Seraphin B and Aranovich J. A 1979 *Solar Energy Conversion, Solid-State Physics Aspects* (Berlin: Springer-Verlag)
- [47] Henry C. H 1980 *Journal of Applied Physics* **51** 4494
- [48] Gjessing J, Sudbø A. S and Marstein E. S 2011 *Journal of Applied Physics* **110** 033104–033104-8
- [49] Brown R and Hwang P 1992 *Introduction to Random Signals and Applied Kalman Filtering* (New York: John Wiley and Sons)
- [50] Mark W. D 1987 *Journal of Sound and Vibration* **119** 451–485
- [51] Palik E 1985 *Handbook of Optical Constants of Solids* (Orlando: Academic)
- [52] Burrese M, Pratesi F, Vynck K, Prasciolu M, Tormen M and Wiersma D. S 2013 *Optics Express* **21** A268–A275

- [53] Pratesi F, Burresi M, Riboli F, Vynck K and Wiersma D. S 2013 *Optics Express* **21** A460–A468
- [54] Vynck K, Burresi M, Riboli F and Wiersma D. S 2012 *Nature Materials* **11** 1017–1022
- [55] Oskooi A, Favuzzi P. A, Tanaka Y, Shigeta H, Kawakami Y and Noda S 2012 *Applied Physics Letters* **100** 181110
- [56] Martins E. R, Li J, Liu Y, Zhou J and Krauss T. F 2012 *Physical Review B* **86** 041404
- [57] Bozzola A, Liscidini M and Andreani L. C 2013 *Progress in Photovoltaics: Research and Applications*
- [58] Martins E. R, Li J, Liu Y, Depauw V, Chen Z, Zhou J and Krauss T. F 2013 *Nature Communications* **4** 2665
- [59] [www.ptci.unamur.be](http://www.ptci.unamur.be)